Life Sciences 234 (2019) 116773

Contents lists available at ScienceDirect

Life Sciences

journal homepage: www.elsevier.com/locate/lifescie

Klotho improves diabetic cardiomyopathy by suppressing the NLRP3 inflammasome pathway

Xuelian Li[a,1], Zhiyang Li[b,1], Bingong Li[a,c,*], Xianjie Zhu[d], Xingjun Lai[c]

[a] Department of Cardiology, Qingdao Municipal Hospital, Qingdao, Shandong 266011, China
[b] Grade 2016 Class 2, The First School of Clinical Medicine, Nanjing Medical University, Nanjing, Jiangsu 211166, China
[c] Department of Cardiology, the First Affiliated Hospital of Nanchang University, Nanchang, Jiangxi 330006, China
[d] Department of Orthopedics, Qingdao Municipal Hospital, Qingdao, Shandong 266011, China

ARTICLE INFO

Keywords:
Diabetic cardiomyopathy
NLRP3
Klotho

ABSTRACT

Aims: NLRP3 inflammasome activation is essential for the development and prognosis of diabetic cardiomyopathy (DCM). The anti-aging protein Klotho is suggested to modulate tissue inflammatory responses. The aim of the present study was to examine the protective effects of Klotho on DCM.

Main methods: A streptozotocin-induced diabetes mouse model was established to assess the effects of Klotho in vivo, which was administered for 12 weeks. The characteristics of type 1 DCM were evaluated by general status, echocardiography, and histopathology. The expression of associated factors was determined by RT-qPCR and western blotting. Parallel experiments to determine the molecular mechanism through which Klotho prevents DCM were performed using H9C2 cells exposed to high glucose (35 mM).

Key findings: Diabetes-induced increases in serum creatine kinase-muscle/brain and lactate dehydrogenase levels, cardiac fibrosis, cardiomyocyte apoptosis, and cardiac dysfunction were ameliorated by Klotho. Additionally, Klotho suppressed TXNIP expression, NLRP3 inflammasome activation, and expression of the inflammatory cytokines tumor necrosis factor α, interleukin-1β, and interleukin-18 in vivo. In high glucose-cultured cardiomyocytes, Klotho and *N*-acetylcysteine significantly downregulated intracellular reactive oxygen species generation and TXNIP/NLRP3 inflammasome activation. Pretreatment of H9C2 cells with NLRP3 siRNA or Klotho prevented high glucose-induced inflammation and apoptosis in H9C2 cells.

Significance: Our results demonstrate that the protective effect of Klotho on diabetes-induced cardiac injury is associated with inhibition of the NLRP3 inflammasome pathway, suggesting its therapeutic potential for DCM.

1. Introduction

Diabetic cardiomyopathy (DCM) significantly contributes to the morbidity and mortality of patients with diabetes, and is characterized by left ventricular hypertrophy, cardiomyocyte apoptosis, interstitial fibrosis, and early diastolic dysfunction, which might be accompanied by systolic dysfunction [1]. Patients with DCM show a progressive decline in heart function over time. The process is irreversible, inevitably leading to end-stage heart failure [2,3]. Additionally, the pathological mechanism of DCM is not completely understood.

Previous studies showed that interleukin-1β (IL-1β) and interleukin-18 (IL-18) are important proinflammatory cytokines for the development of DCM [4]. IL-1β expression levels are consistently increased in the blood or heart tissue of patients with DCM and are clearly correlated with disease severity [5]. IL-1β and IL-18 production is tightly controlled by inflammasome activation. The most extensively studied inflammasome is NLRP3, which is a multiprotein cytoplasmic complex composed of NLRP3, caspase-1, and apoptosis-associated speck-like protein (ASC) [6]. Additionally, several studies suggested that the NLRP3 inflammasome plays a critical role in the inflammatory process of DCM, because silencing of NLRP3 significantly attenuated cardiac dysfunction, myocardial apoptosis, and inflammatory responses induced by diabetes [7]. The mechanisms leading to NLRP3 inflammasome activation remain controversial. One model proposed that NLRP3 is activated by a common pathway involving reactive oxygen species (ROS). A recent report implicated a ROS-sensitive NLRP3 ligand, thioredoxin-interacting protein (TXNIP), in NLRP3 activation. Further, TXNIP and ROS induced NLRP3 activation, leading to maturation of the proinflammatory cytokines IL-1β and IL-18 [8].

Klotho (KL) is a putative anti-aging gene predominantly expressed in

* Corresponding author at: Department of Cardiology, Qingdao Municipal Hospital, Qingdao, Shandong 266011, China.
E-mail address: libingong08@163.com (B. Li).
[1] These authors contributed equally to this work.

https://doi.org/10.1016/j.lfs.2019.116773
Received 20 April 2019; Received in revised form 1 August 2019; Accepted 14 August 2019
Available online 15 August 2019
0024-3205/

the kidney, and its secreted protein functions as a humoral factor to regulate physiological processes [9]. KL has been found to mediate the regulatory effects of calcitonin gene-related peptide during cardiac fibroblast senescence. KL-deficient (kl/+) mice exhibit cardiovascular disease phenotypic features, including accelerated left ventricular hypertrophy and vascular calcification [10,11]. Previous studies demonstrated that KL downregulates inflammatory cytokines and attenuates the generation of ROS in DCM [12]. Although numerous studies have examined the inhibitory roles of KL in inflammatory responses, the effects and underlying mechanisms of KL on DCM remain unclear. This study was conducted to investigate whether KL attenuates the damage associated with experimental DCM, as well as the relevant mechanism.

2. Materials and methods

2.1. Cell culture and treatment

H9C2 cardiomyoblasts were purchased from the Library of Typical Culture of the Chinese Academy of Sciences (Shanghai, China). The cells were cultured in Dulbecco's modified Eagle's medium supplemented with D-glucose (5.5 mmol/L), 10% fetal bovine serum, penicillin (100 U/mL), and streptomycin (100 mg/mL). In the control (Con) group, the medium contained 5.5 mmol/L of D-glucose, and in the high glucose (HG) culture groups, the medium contained 35 mmol/L of D-glucose. *N*-Acetylcysteine (NAC) was obtained from Abcam (Cambridge, UK). KL protein was obtained from R&D Systems (Minneapolis, MN, USA) and dissolved in phosphate-buffered saline (PBS) for in vitro and in vivo experiments.

2.2. Animals

Forty, 6-week-old male C57BL/6 mice (weighing 18–22 g) were purchased from the Laboratory Animal Unit of Nanchang University. Diabetes was induced in the animals via intraperitoneal (i.p.) injection with a single dose of freshly prepared streptozotocin purchased from Sigma-Aldrich (St. Louis, MO, USA; 130 mg/kg) and dissolved in 0.1 mL citrate buffer (pH 4.5). One week later, blood glucose levels were measured using a glucometer (Roche, Basel, Switzerland) after the mice had fasted overnight. Only mice with a fasting blood glucose concentration > 16.7 mmol/L were considered diabetic. Briefly, 1 week after inducing diabetes, diabetic mice (DM) were treated with KL protein (0.01 mg/kg i.p. every 48 h [12]) for 12 weeks. Mice in the DM group were simply treated with vehicle. Blood glucose levels and body weights were measured regularly. After the echocardiography was completed, blood samples were collected, and each mouse heart was removed for further experiments. All animal experiments were conducted according to the Guiding Principles in the Care and Use of Laboratory Animals published by the U.S. National Institutes of Health (NIH Publication No. 8023) and were approved by the Animal Ethics Committee of Nanchang University.

2.3. Determination of cardiac function by echocardiography

An echocardiography system (Sequoia Acuson, Siemens, 15-MHz linear transducer, Erlangen, Germany) was used to measure cardiac function in vivo. The derived echocardiography parameters included left ventricular ejection fraction (LVEF), fractional shortening (FS), and early (E′) to late (A′) diastolic velocity ratio (E′/A′). All measurements represent the mean of five consecutive cardiac cycles.

2.4. Histological analyses

Heart tissues were fixed in 4% paraformaldehyde and then embedded in paraffin. Some tissues were stained with Masson's trichrome to detect collagen. Another portion of the tissue was prepared for immunohistochemical analysis. Heart tissue images were acquired under a light microscope (Leica, Wetzlar, Germany). Image analysis software (Image-Pro Plus 6.0) was used to calculate the collagen volume fraction (CVF = myocardial collagen area/total area of the image) and the average value was determined.

2.5. Measurement of myocardial enzyme activities

The serum cardiac enzyme activities of lactate dehydrogenase (LDH) and creatine kinase-muscle/brain (CK-MB) were determined using a detection kit (Nanjing Jiancheng Bioengineering, Nanjing, China) according to the manufacturer's instructions.

2.6. TUNEL assay

Apoptosis in heart tissue sections was detected using a terminal deoxynucleotidyl transferase dUTP nick-end labeling (TUNEL) detection kit (Roche). TUNEL-positive cells were observed using a fluorescence microscope (Olympus, Tokyo, Japan).

2.7. ELISA

Supernatants of the cell culture or mouse sera were used to measure IL-1β, IL-18, and tumor necrosis factor (TNF)-α (R&D Systems) according to the manufacturer's instructions.

2.8. Flow cytometric analysis

Cell apoptosis was assayed using the fluorescein isothiocyanate (FITC) Annexin V Apoptosis Detection Kit (KeyGEN BioTECH, Nanjing, China) following the manufacturer's instructions. The apoptosis rate was measured by flow cytometry (FACSCanto II; BD, San Jose, CA, USA). PI−/Annexin V−(Q4), PI+/Annexin V−(Q1), PI−/Annexin V+(Q3), and PI+/Annexin V+(Q2) cells were considered viable cells, necrotic cells, early apoptotic cells, and late apoptotic cells, respectively. The apoptosis rate was expressed as Annexin V+/PI− (early apoptosis) and Annexin V+/PI+ (late apoptosis).

2.9. ROS levels

ROS levels were detected with the peroxide-sensitive fluorescent probe 20, 70-dichlorofluorescein diacetate (DCFH-DA) as described previously [13]. The DCF fluorescence of treated cells was detected with a fluorescence microscope (Leica, Germany).

2.10. Assessment of mitochondrial membrane potential (ΔΨm)

ΔΨm was assessed by JC-1 (5,5′,6,6′-tetrachloro-1,1′,3,3′-tetraethyl-imidacarbocyanine iodide, Beyotime, China) staining according to the manufacturer's protocol. Briefly, H9C2 cells were transferred to a slide, washed twice with PBS, and stained with the ΔΨm-specific fluorescent dye JC-1 at 37 °C for 20 min in the dark. Fluorescence was then analyzed with a fluorescence microscope (Leica, Germany).

2.11. siRNA transient transfection

H9C2 cells were transfected with siRNA as previously described [14]. Briefly, H9C2 cells were transfected transiently with NLRP3 siRNA (Shanghai GenePharma Co., Ltd., Shanghai, China) using Lipofectamine 2000 (Invitrogen, Carlsbad, CA, USA) according to the manufacturer's instructions. The target sequence of the NLRP3 siRNA was as follows: 5′-GGTGTTGGAATTAGACAAC-3′. The cells were incubated with KL or HG after siRNA transfection.

2.12. RNA isolation and RT-qPCR analysis

After incubation, total RNA was extracted from the heart tissues and

H9C2 cells using TRIzol (Invitrogen) according to the manufacturer's instructions. Next, 2 μg purified RNA was used to synthesize cDNA using TransScript cDNA Synthesis SuperMix (TransGen Biotech, Beijing, China). Quantitative PCR was performed on a 7300 RealTime PCR System using SYBR Green PCR Master Mix. The following protocol was used for qPCR: 40 cycles (30 s at 95 °C and 10 s at 52 °C) after an initial activation step of 10 min at 95 °C. The specificity of the primers was verified as previously described [15]. The *GAPDH* fragment was amplified as a reference gene. The primer sequences are shown in Table S1.

2.13. Western blot analysis

The isolation of proteins in the cytosol was performed following the method described by Cai et al. [16]. Western blot analysis was utilized as described previously [17]. We used antibodies against TXNIP (1:1000; ab188865, Abcam, Cambridge, UK), NLRP3 (1:1000; ab214185, Abcam, Cambridge, UK), ASC (1:1000; ab70627, Abcam, Cambridge, UK), caspase-1 (1:1000; ab207802, Abcam, Cambridge, UK), IL-1β (1:1000; ab2105, Abcam, Cambridge, UK), α-smooth muscle actin (α-SMA) (1:1000; ab32575, Abcam, Cambridge, UK), Lamin B1 (1:1000; ab133741, Abcam, Cambridge, UK), VDAC1 (1:1000; ab15895, Abcam, Cambridge, UK), cytochrome *c* (1:1000; 11940, Cell Signaling Technology, MA, USA), cleaved-caspase-3 (1:1000; 9661, Cell Signaling Technology, MA, USA), collagen I (1:1000; bs-0578R, Bioss, Beijing, China) collagen III (1:1000; bsm-33129M, Bioss, Beijing, China), and β-actin (1:1000; bsm-33036M, Bioss, Beijing, China). The protein band density was analyzed using an analysis system (Bio-Rad, Hercules, CA, USA). The protein levels were normalized to those of β-actin.

2.14. Statistical analyses

Data are expressed as the means ± SEM of at least three independent experiments. Statistical analysis was performed by one-way analysis of variance followed by a multiple comparisons test with a Bonferroni correction using GraphPad Prism 5 software (GraphPad Software, San Diego, CA, USA). A value of $P < 0.05$ was considered statistically significant.

3. Results

3.1. KL improves serum LDH and CK-MB Levels but fails to attenuate hyperglycemia in diabetic mice

We first established a type 1 diabetic mouse model to investigate the effects of KL in vivo. Blood glucose and body weight of mice were monitored regularly during the period of KL treatment. Consistent with the findings of other investigators, KL had no obvious effects on blood glucose and body weight (Fig. 1A–B). Additionally, in DM, KL treatment prevented the increase in CK-MB and LDH levels, which are generally recognized as biochemical indicators of myocardial injury (Fig. 1C–D).

3.2. KL alleviates cardiac fibrosis in the diabetic heart

We next detected fibrosis and collagen content in diabetic hearts. The collagen fibers and myocardial cells were stained blue and red, respectively, by using Masson's trichrome staining. As shown in Fig. 2A, obvious collagen deposition was observed in the hearts of the DM, whereas KL treatment remarkably mitigated the fibrotic area. Consistently, quantitative analysis showed that the CVF in DM was significantly greater than that in the control and KL groups (Fig. 2B). Moreover, the KL group showed lower levels of types I and III collagen and decreased expression of α-SMA, which is a reliable marker of myofibroblasts, in DM (Fig. 2C). Hematoxylin and eosin (H&E) staining was further used to investigate the protective effect of KL on cardiac remodeling. The DCM mice showed severe damage to the left ventricular ultrastructure including disrupted cellular structures and the infiltration of inflammatory cells (Fig. 2D). After treatment with KL, DM mice showed improved cardiac ultrastructure.

3.3. KL alleviates left-ventricular dysfunction in DM

Transthoracic echocardiography was conducted to evaluate the protective effect of KL on DCM using various cardiac functional parameters including left ventricular fractional shortening (LVFS), LVEF, and (E′/A′) (Fig. 3A). As shown in Fig. 3B–D, compared to that of the control group, DM mice exhibited significantly decreased LVEF, LVFS, and E′/A′, indicating impaired cardiac function. However, KL treatment ameliorated the attenuated LVEF and FS in DM (Fig. 3B–C). With respect to diastolic function, KL increased E′/A′ compared to that ratio in the DM group (Fig. 3D). Collectively, KL treatment ameliorated the impaired cardiac function in the DCM mice.

3.4. KL reduces apoptosis in the hearts of DM mice

DCM is characterized by impaired diastolic myocardial performance and enhanced myocardial apoptosis [18]. To investigate the role of KL in cardiomyocyte apoptosis in DM, a TUNEL assay was performed. TUNEL-positive cardiomyocytes were less frequently observed in the KL group than in the DM group (Fig. 4A–B). We next evaluated the levels of cleaved caspase-3, an apoptosis marker. The results shown in Fig. 4C indicate that the level of cleaved caspase-3 was significantly higher in DM. Furthermore, KL treatment reduced the level of cleaved caspase-3. These results indicate that KL treatment suppresses cardiomyocyte apoptosis in DCM.

3.5. KL attenuates diabetes-stimulated cardiac inflammation in DM by inhibiting the TXNIP/NLRP3 pathway

Considerable evidence supports the fact that the NLRP3 inflammasome contributes to cardiac inflammation in DCM [7,17]. We next evaluated the role of KL in NLRP3 inflammasome activation by immunohistochemical staining, which revealed a marked reduction in cardiac NLRP3 and IL-1β expression in the KL group (Fig. 5A). Moreover, the protein levels of TXNIP, NLRP3, ASC, IL-1β, and cleaved caspase-1 (p20) in the hearts of DM mice were increased (Fig. 5B), whereas KL suppressed activation of the TXNIP/NLRP3 pathway. Consistent with the protein results, the mRNA levels of *NLRP3*, *ASC*, *TXNIP*, *caspase-1*, and *IL-1β* were notably reduced by KL (Fig. 5C–G). Additionally, KL inhibited the levels of mature IL-1β, TNF-α, and IL-18 in the sera of mice (Fig. 5H–J). According to these results, KL prevents NLRP3 inflammasome activation in vivo and attenuates diabetes-induced myocardial injury.

3.6. KL suppresses TXNIP/NLRP3 activation in HG-treated H9C2 cells

To investigate the effect of KL on HG-induced cardiac inflammation, H9C2 cardiomyocytes were pretreated with KL for 1 h and then incubated with HG (35 mM) for 48 h. The control cells were treated with mannitol to eliminate the influence of osmolarity; preliminary results showed that mannitol had no effect (data not shown). Western blotting and RT-qPCR analyses were conducted to analyze the inhibitory effect of KL on the HG-induced expression of inflammasome-related genes (*TXNIP*, *NLRP3*, *IL-1β*, *caspase-1*, and *ASC*) and proteins (NLRP3, ASC, cleaved-caspase-1, IL-1β, and TXNIP). The immunoblotting assay results shown in Fig. 6A revealed that the HG-induced protein expression of NLRP3, ASC, cleaved-caspase-1 (p20), IL-1β, and TXNIP was suppressed by KL. The RT-qPCR results also indicated that the mRNA expression levels of *NLRP3*, *ASC*, *IL-1β*, *caspase-1*, and *TXNIP* were elevated in H9C2 cells treated with HG, whereas the expression of NLRP3 inflammasome and TXNIP was inhibited by KL treatment (Fig. 6B–F).

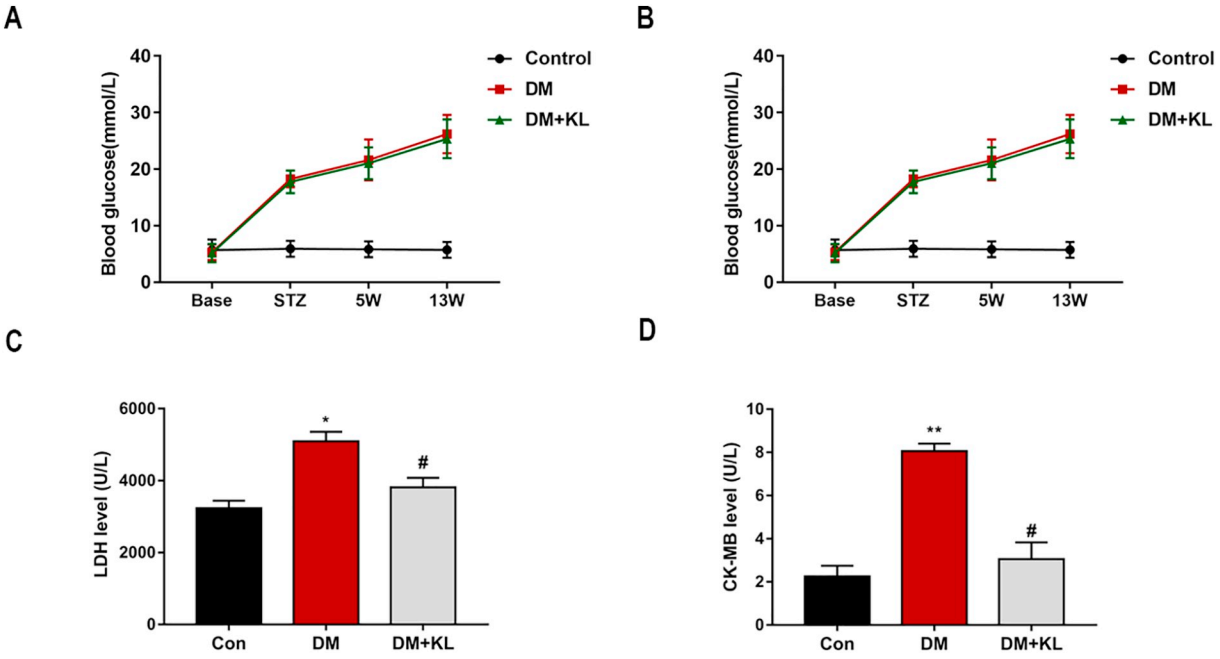

Fig. 1. Effects of Klotho on blood glucose, body weight, and serum LDH and CK-MB levels in diabetic mice.
Blood glucose (A) and body weights (B) at the indicated time points are shown. Serum LDH (C) and CK-MB (D) levels were detected by corresponding detection kits (n = 8–10 per group, $^{*}P < 0.05$, $^{**}P < 0.01$ vs. Con group; #P < 0.05, ##P < 0.01 vs. diabetic mice (DM)).

Moreover, ELISA results revealed that IL-1β, TNF-α, and IL-18 protein levels in the supernatants of H9C2 cell medium were dramatically reduced by KL (Fig. 6G–I). These findings demonstrate that KL treatment suppresses HG-induced TXNIP/NLRP3 activation and its downstream protein expression.

3.7. KL inhibits HG-induced ROS generation in H9C2 cells

To determine the mechanisms underlying these aforementioned effects, we next examined ROS release, a known activator of the NLRP3 inflammasome. H9C2 cells were pretreated with KL or NAC for 1 h and then incubated with HG for 48 h. As shown in Fig. 7A, a significant increase in ROS levels occurred in HG-treated H9C2 cells and KL inhibited this HG-induced ROS generation, which was comparable to the effect induced by treatment with NAC, a known ROS scavenger (Fig. 7A–B). ROS has been reported to trigger the dissociation of TXNIP from thioredoxin, allowing it to bind to NLRP3 [19]. Accordingly, we found that pretreatment with NAC decreased TXNIP expression and IL-1β secretion (Fig. 7C–D). These findings indicate that KL inhibits the TXNIP/NLRP3 pathway by reducing ROS production.

3.8. KL attenuates HG-induced apoptotic death in cardiomyocytes by inhibiting NLRP3 inflammasome in H9C2 cells

KL improved cardiac apoptosis and inhibited NLRP3 inflammasome in DCM mice. However, whether NLRP3 inhibition mediates the protective effects of KL on DCM was unknown. NLRP3 siRNA was used to explore the mechanism through which KL regulates cardiomyocyte apoptosis. Successful transfection was verified by western blotting (Fig. 8A) and the protein levels of cleaved-caspase-1 and IL-1β were shown to be reduced in HG-treated H9C2 cells, suggesting inactivation of the inflammasome. We performed an Annexin V/PI apoptosis assay to detect the level of apoptosis in H9C2 cells after different treatments. Here, annexin V-positive cells, including both early (AV + /PI-) and late (AV + /PI +) apoptotic cells, were considered apoptotic cells. Fig. 8B and C revealed that NLRP3 knockdown significantly decreased the number of early apoptotic H9C2 cells after HG treatment, which was comparable to the effect induced by KL. At the same time, the rate of late apoptosis of H9C2 cells after NLRP3 knockdown or KL treatment was significantly decreased relative to that of HG-treated H9C2 cells (Fig. 8D). Moreover, pretreatment of H9C2 cells with NLRP3 siRNA or KL significantly inhibited the HG-induced increase in cleaved-caspase-3 in H9C2 cells (Fig. 8E). Mitochondrial dysfunction leads to diminished energy generation, loss of myocyte contractility, altered electrical properties, and eventual cardiomyocyte apoptosis, which involves ΔΨm loss and cytochrome *c* release. JC-1 staining was performed to measure the stability of ΔΨm in H9C2 cells. As shown in Fig. 8F, HG significantly decreased ΔΨm, as evidenced by the decreased aggregate-to-monomer ratio of JC-1. Pretreatment of H9C2 cells with NLRP3 siRNA or KL effectively nullified this HG-induced decrease in ΔΨm (Fig. 8F–G). Moreover, western blot results revealed that cytochrome *c* levels in the cytoplasm were higher in the HG group than in the Con group. Pretreatment of H9C2 cells with NLRP3 siRNA or KL inhibited the HG-stimulated cytochrome *c* release (Fig. 8H).

4. Discussion

Diabetes increases the risk of heart disease, and 50% of people with diabetes die of cardiovascular disease [5]. Cell inflammation is a closely related key factor in the pathogenesis of DCM [20]. Strategies for inhibiting dysregulated inflammation in DCM patients have attracted increasing attention in recent years. *KL*, a novel anti-senescence gene, is closely associated with age-related diseases, such as chronic renal failure and cardiovascular diseases [21–24]. The main type of KL protein is called α-KL (KL). The *KL* gene has been reported to encode two other KL proteins, β-KL and Klotho-related protein (Klrp) [25–27]. There are two types of soluble α-KL protein, namely shedded and secreted α-KL. α-KL has extensive functions, which are partially due to the secreted form that circulates in the blood. The α-KL protein is also highly homologous across species. In particular, the α-KL protein sequence is 98% identical between humans and mice [27]. Our study mainly investigated the effect of circulating soluble mouse KL. A recent study showed that KL prevents diabetic myocardial damage by preventing inflammatory responses and oxidative stress [12]. Nie et al. have suggested that serum levels of α-KL and β-KL among patients with T2DM were positively correlated with creatinine clearance rate and

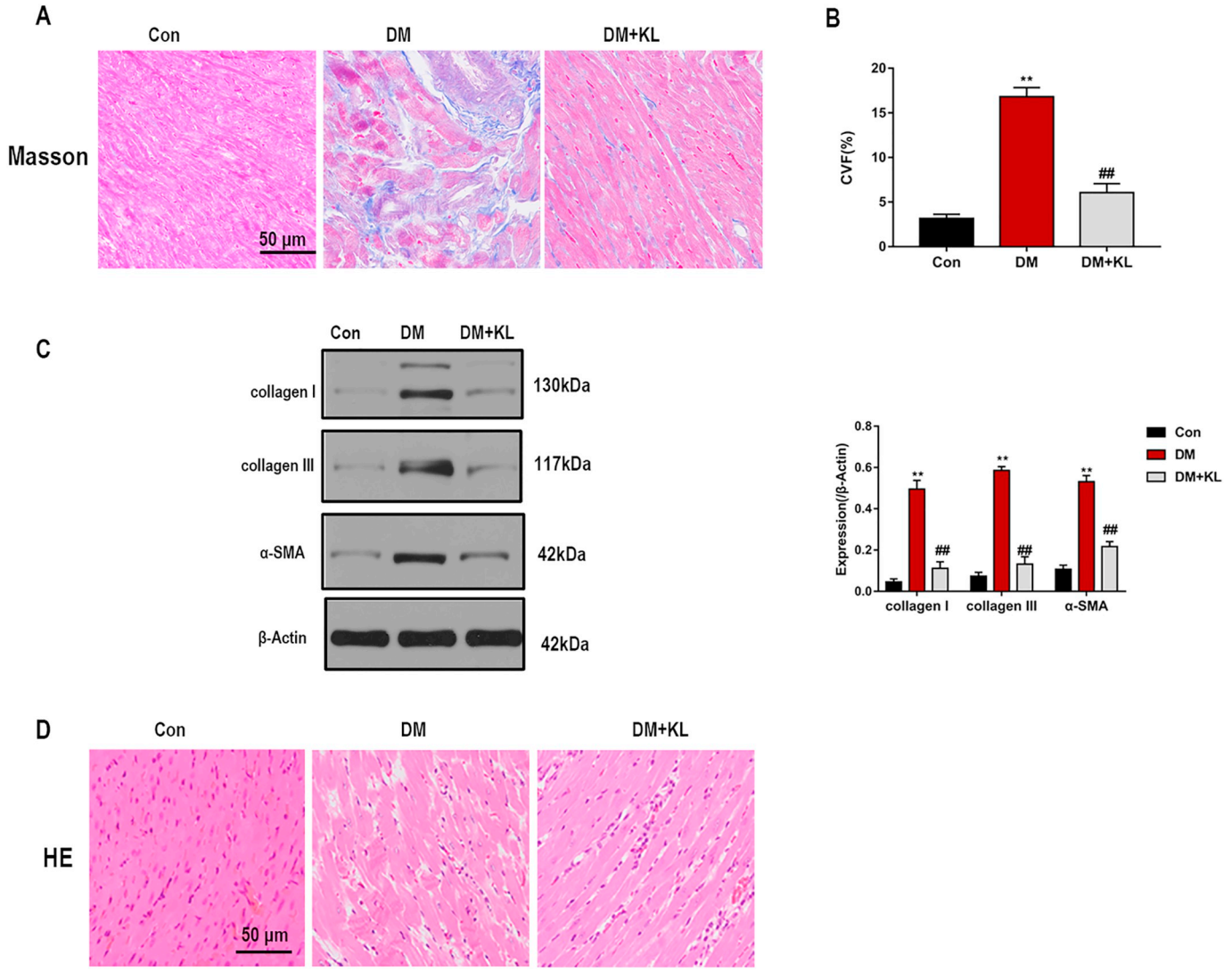

Fig. 2. Klotho prevents cardiac fibrosis and histological abnormalities in diabetic hearts.
(A) Representative Masson's trichrome staining. (B) Comparison of collagen volume fraction (CVF) in mice from each group. (C) Expression of collagen I, collagen III, and α-SMA in heart tissue assayed by western blot. (D) Heart tissues in each group were stained with hematoxylin and eosin (H&E) (n = 8–10 per group, $*P < 0.05$, $**P < 0.01$ vs. Con group; #P < 0.05, ##P < 0.01 vs. diabetic mice (DM)).

negatively correlated with urinary albumin to creatinine ratio, serum creatinine, blood urea nitrogen, and glucose levels [28]. The protective role of KL in DCM is emerging, but the underlying mechanisms remain unclear. In this study, we showed that inhibition of the NLRP3 inflammasome is essential for the KL-mediated protective effects in DCM. Mice with diabetes showed impaired cardiac functions, accelerated cardiac fibrosis and cell death. The NLRP3 inflammasome and its potential activator, TXNIP, were induced in vivo, which was inhibited by KL treatment. KL had a beneficial effect on the functional and structural alterations in DCM but had no effect on the levels of blood glucose, suggesting that the protective effect of KL was associated with its anti-inflammatory properties rather than the regulation of blood glucose metabolism. To explore the mechanism underlying the protective effect of KL on DCM, we performed experiments in vitro. In our study, we found that KL reversed HG-induced NLRP3 inflammasome activation. Additionally, KL significantly reduced HG-induced ROS generation, and scavenging ROS with NAC attenuated TXNIP expression and inflammation in HG-treated H9C2 cells. These results indicate that KL inhibits the TXNIP/NLRP3 inflammasome pathway by degrading ROS in HG-treated H9C2 cells. Furthermore, we showed the anti-apoptotic effect of KL in H9C2 cells, effects that also occurred with knockdown of NLRP3. These findings suggest that KL ameliorates HG-induced cardiomyocyte injury by inhibiting the NLRP3 inflammasome.

The activated NLRP3 inflammasome regulates the conversion of pro-IL-1β into its mature form, which exacerbates inflammation and tissue damage. IL-1β expression was observed in the heart tissues of DCM patients, whereas inhibition of IL-1β protected cells from apoptosis [29,30]. The serum levels of TNF-α and IL-1β were also found to be markedly increased in hyperglycemia-induced myocardial injury [31]. Recently, a study showed that the NLRP3 inflammasome is responsible for the glucotoxicity-related cardiac inflammation during the process of DCM [7]. Consistent with the results of a previous study [32], the present study showed that the NLRP3 inflammasome and its downstream cytokines including mature IL-1β, TNF-α, and IL-18 were increased both in vivo and in vitro.

Several cellular signals are responsible for NLRP3 inflammasome activation including cytosolic K^+ efflux, ROS production, and mitochondrial DNA release [33]. Among these factors, ROS overproduction is thought to be an important upstream event for activating NLRP3 inflammasome and stimulating IL-1β production [34].

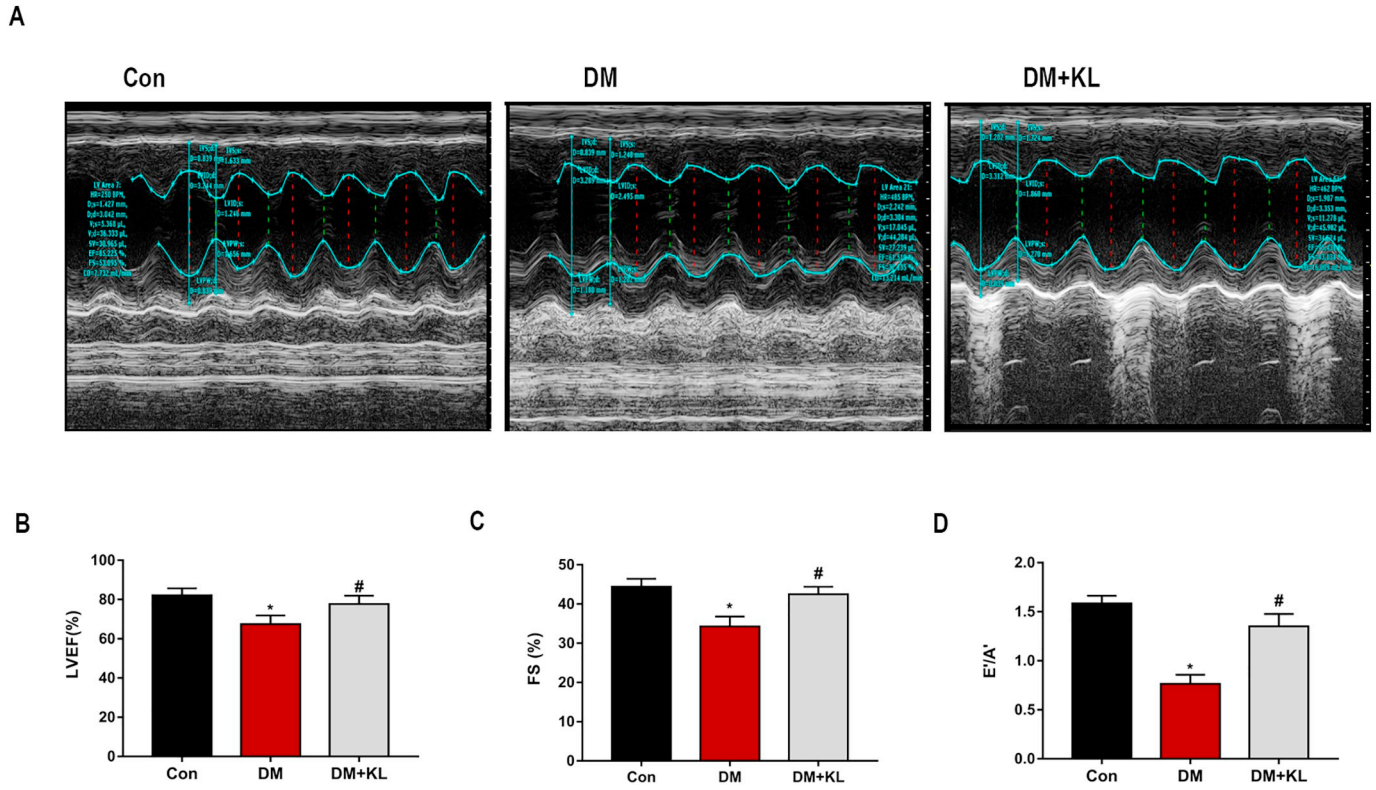

Fig. 3. Klotho alleviates diabetes-induced left ventricular dysfunction.
(A) Representative images of M-mode echocardiograms in each group. Evaluations of left ventricular ejection fraction (LVEF) (B), fractional shortening (FS) (C), and early (E′) to late (A′) diastolic velocity ratio (E′/A′) (D) (n = 8–10 per group, $*P < 0.05$, $**P < 0.01$ vs. Con group; #P < 0.05, ##P < 0.01 vs. diabetic mice (DM)).

Hyperglycemia-induced ROS generation acts as an important contributor to NLRP3 inflammasome activation in the diabetic myocardium [19]. Additionally, ROS inhibitors dramatically reduce the secretion of mature IL-1β and IL-18 [32]. Hyperglycemia was also found to increase the production of ROS, leading to the dissociation of thioredoxin and the TXNIP complex [35]. Subsequently, TXNIP binds to the leucine-rich repeat region of NLRP3, leading to NLRP3 inflammasome activation [36]. NLRP3 agonists trigger the production of ROS,

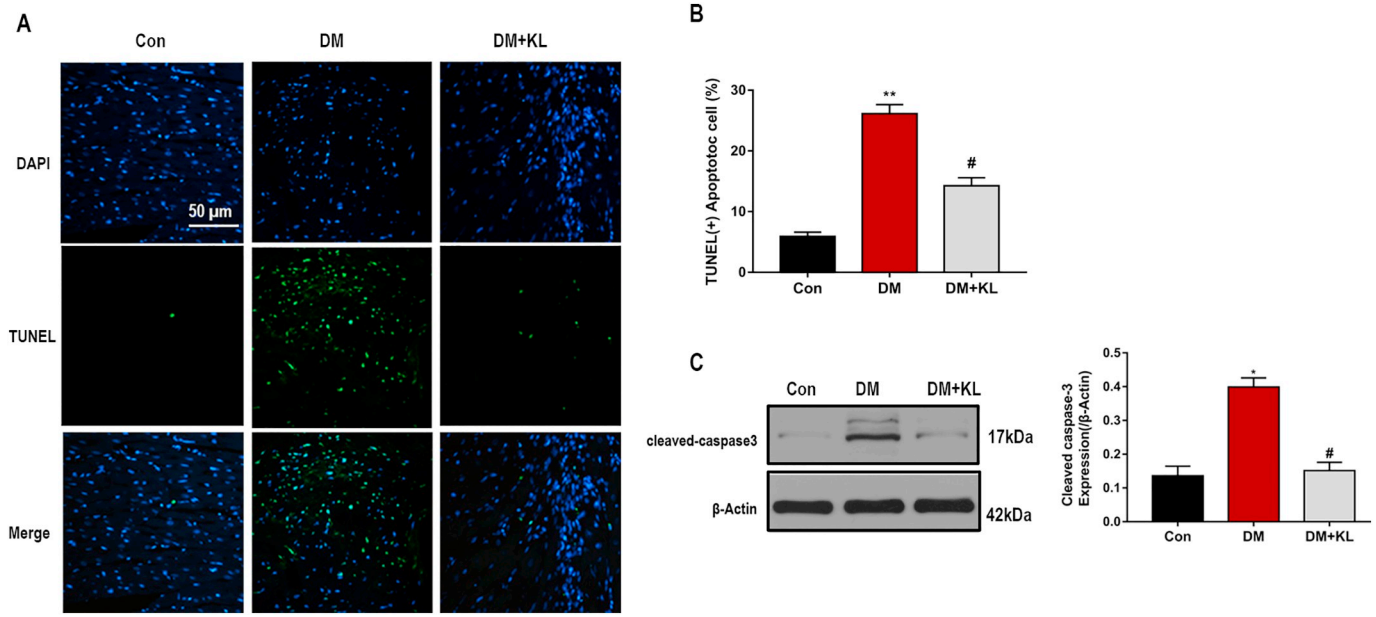

Fig. 4. Klotho inhibits cardiomyocyte apoptosis in diabetic mice (DM).
(A) Representative TUNEL-positive cells (green) in heart tissues of DM. (B) Quantitative analysis of apoptotic cardiomyocytes isolated from cardiac tissues. (C) Expression of cleaved-caspase-3 in the heart tissue assayed by western blot (n = 8–10 per group, *P < 0.05, **P < 0.01 vs. Con group; #P < 0.05, ##P < 0.01 vs. DM).

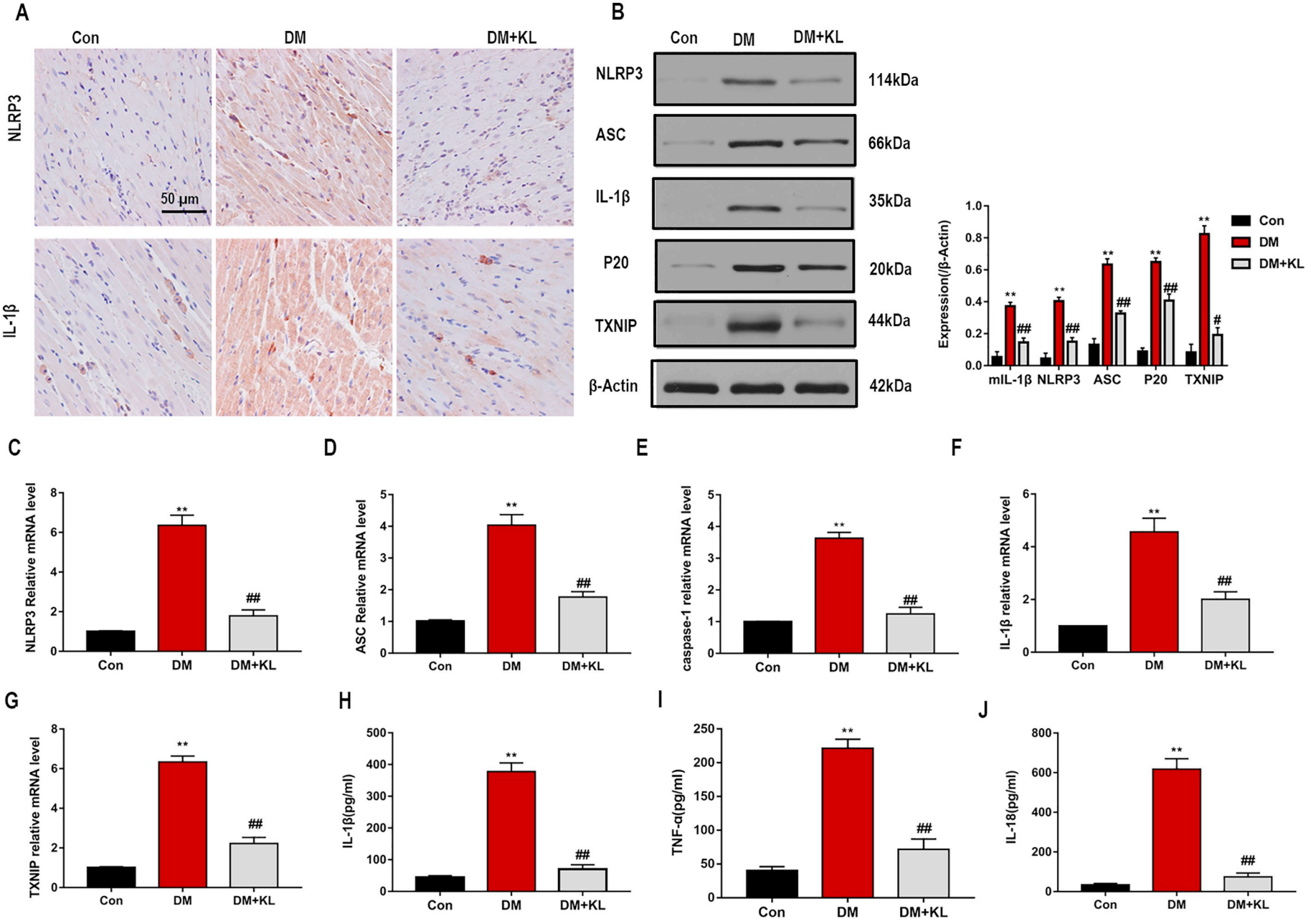

Fig. 5. Klotho attenuates NLRP3 inflammasome activation in the diabetic mouse model.
(A) Representative immunohistochemical staining for IL-1β and NLRP3 expression in heart tissues. (B) Expression of NLRP3, ASC, IL-1β, cleaved-caspase-1 (p20), and TXNIP in heart tissues assayed by western blotting. mRNA levels of *NLRP3* (C), *ASC* (D), *caspase-1* (E), *IL-1β* (F), and *TXNIP* (G) were assayed by RT-qPCR in myocardial tissue. ELISA results showing serum levels of IL-1β (H), TNF-α (I), and IL-18 (J) in the study groups (n = 8–10 per group, $^{*}P < 0.05$, $^{**}P < 0.01$ vs. Con group; #P < 0.05, ##P < 0.01 vs. diabetic mice (DM)).

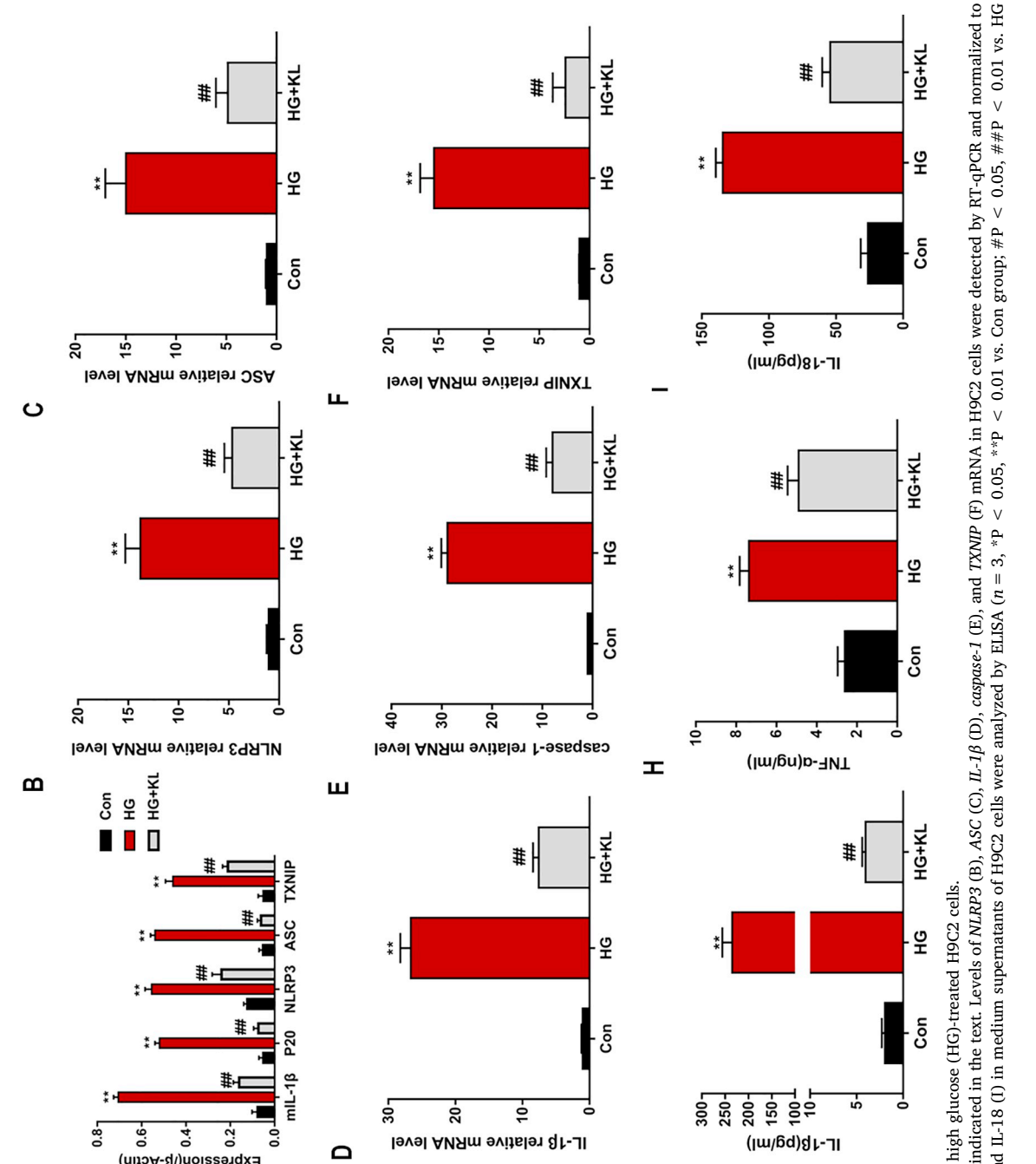

Fig. 6. Klotho inhibits NLRP3 inflammasome activation in high glucose (HG)-treated H9C2 cells.
(A) H9C2 cell lysates were analyzed by immunoblotting as indicated in the text. Levels of *NLRP3* (B), *ASC* (C), *IL-1β* (D), *caspase-1* (E), and *TXNIP* (F) mRNA in H9C2 cells were detected by RT-qPCR and normalized to those of *GAPDH*. Protein levels of IL-1β (G), TNF-α (H), and IL-18 (I) in medium supernatants of H9C2 cells were analyzed by ELISA ($n = 3$, *P < 0.05, **P < 0.01 vs. Con group; #P < 0.05, ##P < 0.01 vs. HG group).

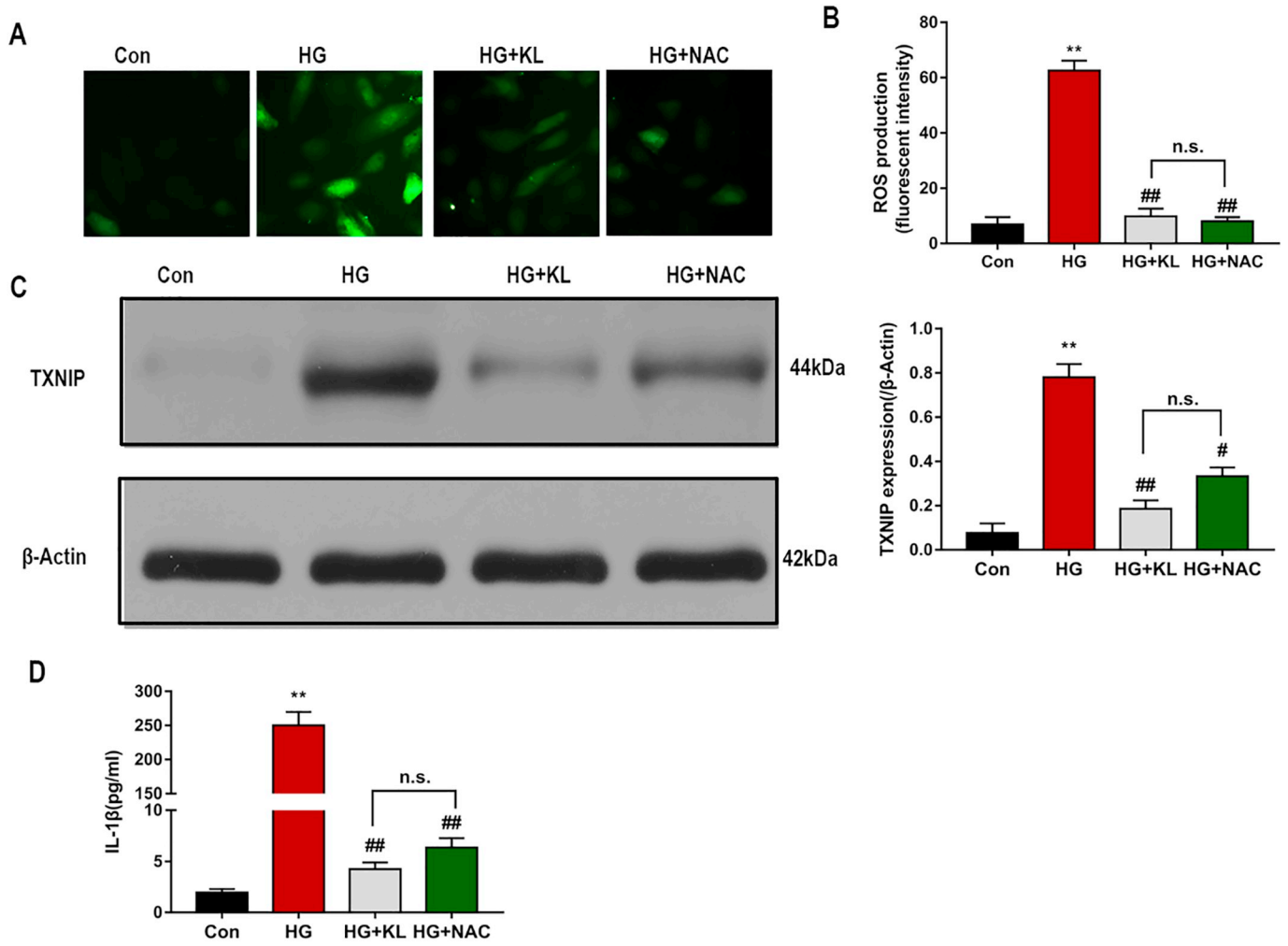

Fig. 7. Klotho inhibits high glucose (HG)-induced reactive oxygen species (ROS) production in H9C2 cells.
(A) Detection of ROS in various groups by DCFH-DA probes and representative images acquired under a fluorescence microscope. Green fluorescence intensity reflects the presence of ROS. (B) Comparison of ROS levels across different treatment groups. (C) Relative TXNIP protein levels in lysates of H9C2 cells were determined by western blotting and normalized to those of β-actin. (D) Protein levels of IL-1β in medium supernatants of H9C2 cells were analyzed by ELISA (n = 3, *P < 0.05, **P < 0.01 vs. Con group; #P < 0.05, ##P < 0.01 vs. HG group).

leading to activation of the NLRP3 inflammasome via the ROS-sensitive TXNIP protein [37]. TXNIP might be the link between the glucose signal and NLRP3 activation in DCM [38]. We found that KL downregulates ROS production and prevents TXNIP expression, which contribute to inhibition of NLRP3 inflammasome in response to high-glucose challenge.

Cell apoptosis is a defining pathological feature of DCM, which leads to decreased myocardial contractility. Hyperglycemia can directly induce the release of cytochrome *c* from the mitochondria into the cytoplasm, triggering a cascade activation of caspase-3 and leading to the intrinsic apoptosis of cardiomyocytes [39]. Our results also showed that HG induced an obvious loss of ΔΨm, cytochrome *c* release, caspase-3 activation, and subsequent apoptosis. These abnormalities drive the development of diabetic cardiac hypertrophy and heart failure. Interestingly, NLRP3 inflammasome activation and the resulting cytokine release promote apoptosis, further exacerbating the severity of DCM [40]. A recent study also demonstrated that an NLRP3-specific inflammasome inhibitor significantly improved cardiac apoptosis [32]. Moreover, inhibiting the activation of NLRP3 significantly reduced the apoptosis of hemin-treated endothelial cells [41]. Collectively, these results suggest that the NLRP3 inflammasome contributes to diabetes-induced cardiac injury. Consistently, treatment with KL markedly attenuates cardiac injury and decreases NLRP3 inflammasome activation both in vivo and in vitro. Additionally, the pretreatment of H9C2 cells with NLRP3 siRNA or KL attenuates the activation of cardiac apoptosis that is associated with DCM. However, the relevant evidence of how NLRP3 effectively regulates cardiac apoptosis is absent in this study. Future studies are required to investigate the mechanistic details of KL in modulating the cardiomyocyte apoptosis and the expression of NLRP3 inflammasome.

5. Conclusion

In conclusion, through in vitro and in vivo studies, we demonstrated that KL might have significant therapeutic potential for treating DCM. Further, the beneficial effect of KL was found to be dependent on inhibition of the NLRP3 inflammasome.

Supplementary data to this article can be found online at https://doi.org/10.1016/j.lfs.2019.116773.

Author contributions

Xuelian Li and Bingong Li contributed to study conception and design, acquisition of data, analysis and interpretation of data, and manuscript writing; Zhiyang Li and Xianjie Zhu contributed to data collection and analysis, Xingjun Lai contributed to manuscript writing.

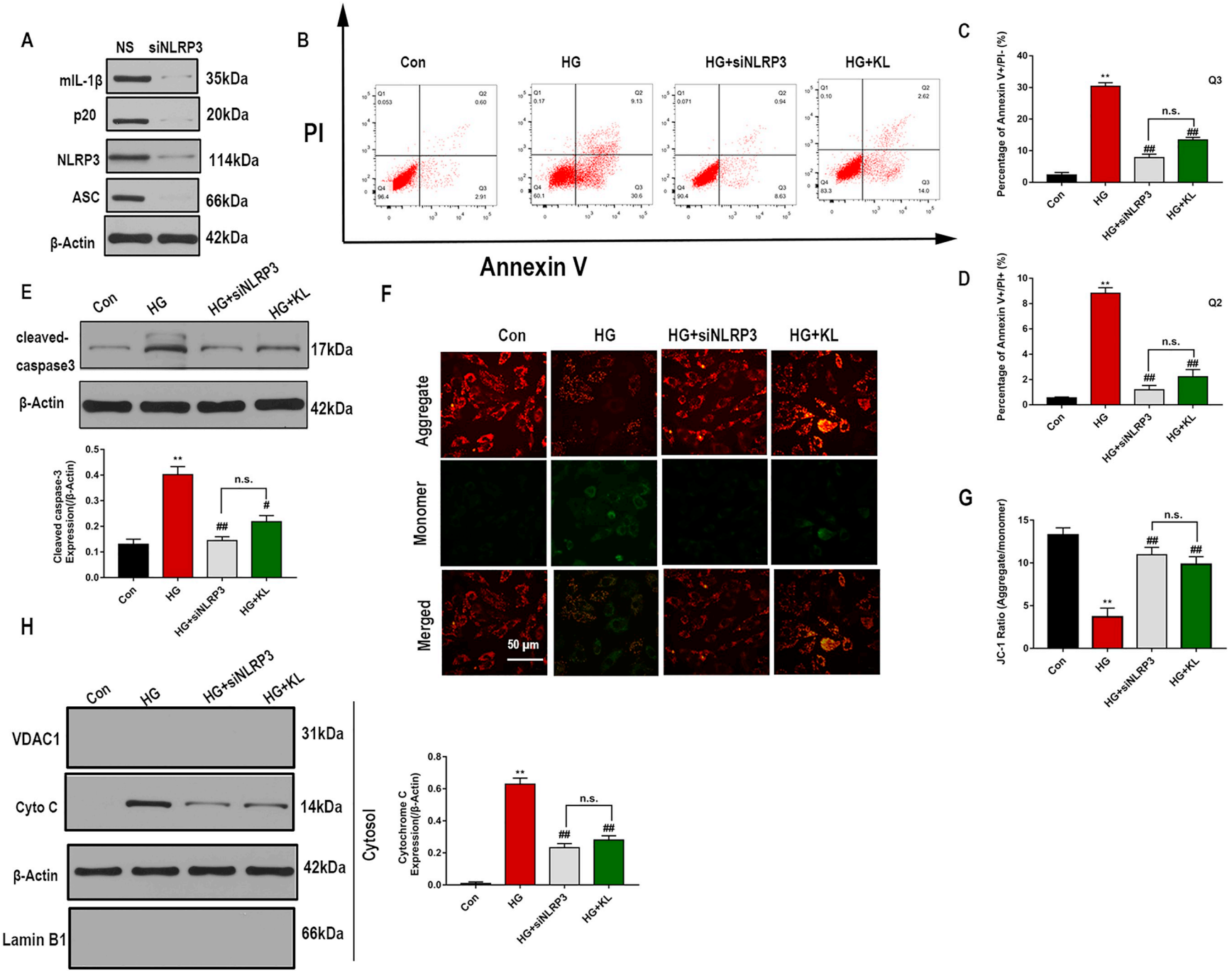

(caption on next page)

Fig. 8. Klotho exerts its effect on apoptosis by inhibiting NLRP3 inflammasome in H9C2 cells.
H9C2 cells were transfected with NLRP3 siRNA. At 12 h post-transfection, cells were treated with high glucose (HG; 35 mM) in the presence or absence of Klotho (400 pM) for 48 h. NS, non-specific siRNA; siNLRP3, NLRP3 siRNA; Con, control. (A) Western blot analysis revealed successful knockdown of NLRP3 (*P < 0.05, **P < 0.01 vs. NS). (B) Apoptotic cells were detected by flow cytometry; the histogram shows the percentages of (C) early apoptotic cells (PI−/Annexin V+) and (D) late apoptotic cells (PI+/Annexin V+). (E) Relative cleaved-caspase-3 protein levels in lysates of H9C2 cells were measured by western blot and normalized to those of β-actin. (F) Representative images of JC-1 staining of mitochondrial membrane potential in H9C2 cells. (G) Quantitative analysis of mitochondrial membrane potential (ratio of red fluorescence obtained at 590 nm to green fluorescence at 530 nm) in H9C2 cells. (H) The cytoplasm of H9C2 cells was analyzed by immunoblotting for cytochrome *c*; anti-VDAC1 and anti-Lamin B1 were used to confirm the absence of contaminating proteins from mitochondrial and nuclear compartments, respectively. (n = 3, *P < 0.05, **P < 0.01 vs. Con group; #P < 0.05, ##P < 0.01 vs. HG group).

All authors read and approved the final manuscript.

Declaration of competing interest

The authors declare that there are no conflicts of interest.

Acknowledgments

This work was supported by the National Natural Science Foundation of China [grant number 81860052].

References

[1] S. Boudina, E.D. Abel, Diabetic cardiomyopathy, causes and effects [J], Rev. Endocr. Metab. Disord. 11 (1) (2010) 31–39.
[2] H. Wei, H. Qu, H. Wang, et al., 1,25-Dihydroxyvitamin-D3 prevents the development of diabetic cardiomyopathy in type 1 diabetic rats by enhancing autophagy via inhibiting the beta-catenin/TCF4/GSK-3beta/mTOR pathway[J], J. Steroid Biochem. Mol. Biol. 168 (2017) 71–90.
[3] W. Liu, A. Ruiz-Velasco, S. Wang, et al., Metabolic stress-induced cardiomyopathy is caused by mitochondrial dysfunction due to attenuated Erk5 signaling[J], Nat. Commun. 8 (1) (2017) 494.
[4] R.S. Guleria, A.B. Singh, I.T. Nizamutdinova, et al., Activation of retinoid receptor-mediated signaling ameliorates diabetes-induced cardiac dysfunction in Zucker diabetic rats [J], J. Mol. Cell. Cardiol. 57 (2013) 106–118.
[5] B.R. Goyal, A.A. Mehta, Diabetic cardiomyopathy: pathophysiological mechanisms and cardiac dysfuntion[J], Hum. Exp. Toxicol. 32 (6) (2013) 571–590.
[6] M. Lamkanfi, T.D. Kanneganti, Nlrp3: an immune sensor of cellular stress and infection [J], Int. J. Biochem. Cell Biol. 42 (6) (2010) 792–795.
[7] B. Luo, B. Li, W. Wang, et al., NLRP3 gene silencing ameliorates diabetic cardiomyopathy in a type 2 diabetes rat model[J], PLoS One 9 (8) (2014) e104771.
[8] K. Schroder, J. Tschopp, The inflammasomes[J], Cell 140 (6) (2010) 821–832.
[9] Y. Takahashi, -O M Kuro, F. Ishikawa, Aging mechanisms [J], Proc. Natl. Acad. Sci. U. S. A. 97 (23) (2000) 12407–12408.
[10] K. Lim, T.S. Lu, G. Molostvov, et al., Vascular klotho deficiency potentiates the development of human artery calcification and mediates resistance to fibroblast growth factor 23[J], Circulation 125 (18) (2012) 2243–2255.
[11] K. Yang, C. Wang, L. Nie, et al., Klotho protects against Indoxyl Sulphate-induced myocardial hypertrophy [J], J. Am. Soc. Nephrol. 26 (10) (2015) 2434–2446.
[12] Y. Guo, X. Zhuang, Z. Huang, et al., Klotho protects the heart from hyperglycemia-induced injury by inactivating ROS and NF-kappaB-mediated inflammation both in vitro and in vivo[J], Biochim. Biophys. Acta Mol. Basis Dis. 1864 (1) (2018) 238–251.
[13] E. Liang, X. Liu, Z. Du, et al., Andrographolide ameliorates diabetic cardiomyopathy in mice by blockage of oxidative damage and NF-kappaB-mediated inflammation [J], Oxidative Med. Cell. Longev. 2018 (2018) 9086747.
[14] L. Hu, S. Zhang, H. Wen, et al., Melatonin decreases M1 polarization via attenuating mitochondrial oxidative damage depending on UCP2 pathway in prorenin-treated microglia[J], PLoS One 14 (2) (2019) e212138.
[15] B.L. Liu, Y.P. Chen, H. Cheng, et al., The protective effects of curcumin on obesity-related Glomerulopathy are associated with inhibition of Wnt/beta-catenin signaling activation in podocytes[J], Evid. Based Complement. Alternat. Med. 2015 (2015) 827472.
[16] H.A. Cai, X. Tao, L.J. Zheng, et al., Ozone alleviates ischemia-reperfusion injury by inhibiting mitochondrion-mediated apoptosis pathway in SH-SY5Y cells[J], Cell Biol. Int. (2018), https://doi.org/10.1002/cbin.11087.
[17] X. Zhang, X. Ma, M. Zhao, et al., H2 and H3 relaxin inhibit high glucose-induced apoptosis in neonatal rat ventricular myocytes[J], Biochimie 108 (2015) 59–67.
[18] X. Zhang, L. Pan, K. Yang, et al., H3 Relaxin protects against myocardial injury in experimental diabetic cardiomyopathy by inhibiting myocardial apoptosis, fibrosis and inflammation[J], Cell. Physiol. Biochem. 43 (4) (2017) 1311–1324.
[19] W. Luo, Y. Jin, G. Wu, et al., Blockage of ROS and MAPKs-mediated inflammation via restoring SIRT1 by a new compound LF10 prevents type 1 diabetic cardiomyopathy[J], Toxicol. Appl. Pharmacol. 370 (2019) 24–35.
[20] M. Savi, L. Bocchi, P. Mena, et al., In vivo administration of urolithin a and B prevents the occurrence of cardiac dysfunction in streptozotocin-induced diabetic rats [J], Cardiovasc. Diabetol. 16 (1) (2017) 80.
[21] L.M. Zhang, J. Zhang, Y. Zhang, et al., Interleukin-18 promotes fibroblast senescence in pulmonary fibrosis through down-regulating klotho expression [J], Biomed. Pharmacother. 113 (2019) 108756.
[22] W.Q. Li, S.L. Tan, X.H. Li, et al., Calcitonin gene-related peptide inhibits the cardiac fibroblasts senescence in cardiac fibrosis via up-regulating klotho expression [J], Eur. J. Pharmacol. 843 (2019) 96–103.
[23] M. Ullah, Z. Sun, Klotho deficiency accelerates stem cells aging by impairing telomerase activity [J], J. Gerontol. A Biol. Sci. Med. Sci. (2018), https://doi.org/10.1093/gerona/gly261.
[24] M.C. Izquierdo, M.V. Perez-Gomez, M.D. Sanchez-Nino, et al., Klotho, phosphate and inflammation/ageing in chronic kidney disease[J], Nephrol. Dial. Transplant. 27 (Suppl. 4) (2012) v6–v10.
[25] K. Yahata, K. Mori, H. Arai, et al., Molecular cloning and expression of a novel klotho-related protein[J], J. Mol. Med. (Berl) 78 (7) (2000) 389–394.
[26] S. Ito, T. Fujimori, A. Furuya, et al., Impaired negative feedback suppression of bile acid synthesis in mice lacking betaKlotho[J], J. Clin. Invest. 115 (8) (2005) 2202–2208.
[27] Y. Matsumura, H. Aizawa, T. Shiraki-Iida, et al., Identification of the human klotho gene and its two transcripts encoding membrane and secreted klotho protein[J], Biochem. Biophys. Res. Commun. 242 (3) (1998) 626–630.
[28] F. Nie, D. Wu, H. Du, X. Yang, M. Yang, X. Pang, et al., Serum klotho protein levels and their correlations with the progression of type 2 diabetes mellitus, J. Diabetes Complicat. 31 (2017) 594–598.
[29] E. Westphal, S. Rohrbach, M. Buerke, et al., Altered interleukin-1 receptor antagonist and interleukin-18 mRNA expression in myocardial tissues of patients with dilatated cardiomyopathy[J], Mol. Med. 14 (1–2) (2008) 55–63.
[30] X. Yang, F. Lu, L. Li, et al., Wu-Mei-wan protects pancreatic beta cells by inhibiting NLRP3 Inflammasome activation in diabetic mice [J], BMC Complement. Altern. Med. 19 (1) (2019) 35.
[31] W. Zheng, D. Li, X. Gao, et al., Carvedilol alleviates diabetic cardiomyopathy in diabetic rats [J], Exp. Ther. Med. 17 (1) (2019) 479–487.
[32] H. Zhang, X. Chen, B. Zong, et al., Gypenosides improve diabetic cardiomyopathy by inhibiting ROS-mediated NLRP3 inflammasome activation[J], J. Cell. Mol. Med. 22 (9) (2018) 4437–4448.
[33] M. Lamkanfi, V.M. Dixit, Mechanisms and functions of inflammasomes[J], Cell 157 (5) (2014) 1013–1022.
[34] L.L. Qiu, M.H. Ji, H. Zhang, et al., NADPH oxidase 2-derived reactive oxygen species in the hippocampus might contribute to microglial activation in postoperative cognitive dysfunction in aged mice[J], Brain Behav. Immun. 51 (2016) 109–118.
[35] L. Minutoli, D. Puzzolo, M. Rinaldi, et al., ROS-mediated NLRP3 Inflammasome activation in brain, heart, kidney, and testis ischemia/reperfusion injury[J], Oxidative Med. Cell. Longev. 2016 (2016) 2183026.
[36] H.H. Tseng, C.T. Vong, Y.W. Kwan, et al., TRPM2 regulates TXNIP-mediated NLRP3 inflammasome activation via interaction with p47 phox under high glucose in human monocytic cells [J], Sci. Rep. 6 (2016) 35016.
[37] K. Schroder, R. Zhou, J. Tschopp, The NLRP3 inflammasome: a sensor for metabolic danger? [J], Science 327 (5963) (2010) 296–300.
[38] B. Luo, B. Li, W. Wang, et al., Rosuvastatin alleviates diabetic cardiomyopathy by inhibiting NLRP3 inflammasome and MAPK pathways in a type 2 diabetes rat model[J], Cardiovasc. Drugs Ther. 28 (1) (2014) 33–43.
[39] J. Zheng, J. Cheng, S. Zheng, et al., Physical exercise and its protective effects on diabetic cardiomyopathy: what is the evidence? Front. Endocrinol. (Lausanne) 9 (2018) 729.
[40] F. Yang, Y. Qin, J. Lv, et al., Silencing long non-coding RNA Kcnq1ot1 alleviates pyroptosis and fibrosis in diabetic cardiomyopathy[J], Cell Death Dis. 9 (10) (2018) 1000.
[41] F. Xu, G. Shen, Z. Su, et al., Glibenclamide ameliorates the disrupted blood-brain barrier in experimental intracerebral hemorrhage by inhibiting the activation of NLRP3 inflammasome, Brain Behav (2019) e1254, , https://doi.org/10.1002/brb3.1254.